# Small-Angle Neutron Scattering Analysis of Bottlebrush Polymers Prepared via Grafting-Through Polymerization

Stacy L. Pesek,[†] Xianyu Li,[†] Boualem Hammouda,[‡] Kunlun Hong,[§] and Rafael Verduzco*,[†]

[†]Chemical and Biomolecular Engineering Department, Rice University, Houston, Texas 77251-1892, United States
[‡]NIST Center for Neutron Research, Gaithersburg, Maryland 20899-8562, United States
[§]Center for Nanophase Materials Sciences, Oak Ridge National Laboratory, Oak Ridge, Tennessee 37831-6494, United States

Ⓢ *Supporting Information*

ABSTRACT: Bottlebrush polymers are highly branched macromolecules with potential applications in antifouling coatings, rheological modifiers, and drug delivery systems. However, the solution conformation of bottlebrush polymers has been studied in only a limited set of materials made primarily by grafting-from polymerization. Here we present small-angle neutron scattering (SANS) measurements on a series of polystyrene bottlebrush polymers with varying side-chain and backbone lengths in d_8-toluene to analyze their size, shape, and conformation. Bottlebrush polymers with 2−7 kg mol^{-1} polystyrene side chains (degree of polymerization DP = 14−54) and poly(oxanorbornene) backbones (DP = 10−264) were synthesized using reversible addition−fragmentation chain transfer (RAFT) followed by a ring-opening metathesis polymerization (ROMP) grafting-through synthesis scheme. Analysis by Guinier−Porod, rigid cylinder, and flexible cylinder models provided estimates of the bottlebrush polymer length, radius, and stiffness. The bottlebrush polymer cross-sectional area depends primarily on side-chain DP, and the radius of gyration R_g exhibits a power-law dependence with side-chain DP. We also observe a sphere-to-cylinder transition with increasing backbone DP, with the transition occurring at a backbone DP of approximately 120 for the polystyrene bottlebrush polymers studied. The maximum molecular dimension for the series studied varies from 25 to 350 nm.
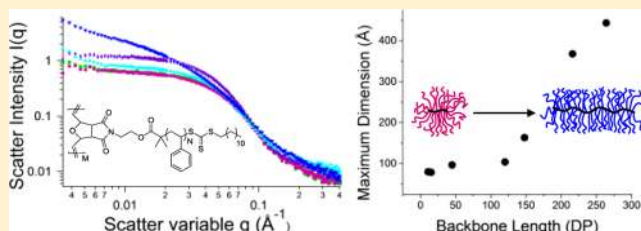
■ INTRODUCTION

Bottlebrush polymers are highly branched macromolecules with polymeric side chains attached to a main-chain polymer backbone (Figure 1) and are promising for applications that
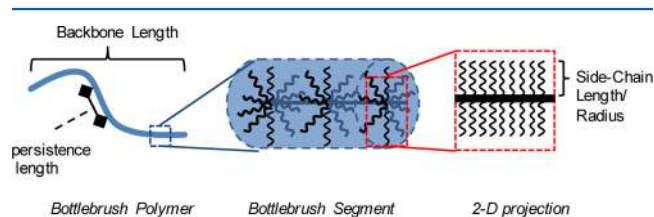

Figure 1. Schematic of a bottlebrush polymer, depicting an extended, cylindrical bottlebrush polymer with fully stretched polymeric side-chains.

rely on large, highly extended macromolecules and/or densely packed polymeric chains. These include stimuli-responsive surfaces, polymer photonics, and drug delivery systems.[1−8] The development of bottlebrush polymers for applications such as drug delivery requires quantitative knowledge of their structure in solution, but the majority of work with bottlebrush polymers has relied on the characterization of bottlebrush polymers adsorbed on a surface or in the melt state. This can provide an estimate of the single-molecule size but not quantitative

information on their solution-state structure. Here, we present a detailed analysis of the conformation of a model series of bottlebrush polymers in solution through small-angle neutron scattering (SANS) measurement and analysis.

Three general techniques to synthesize bottlebrush polymers include grafting-from,[9−12] grafting-to,[13,14] and grafting-through.[2,15−17] The grafting-from approach has been the most widely used[15,18,19] and can give large, synthetically diverse bottlebrush polymers but with imperfect side-chain attachment.[9,12,20] The grafting-to technique yields varying degrees of grafting efficiencies.[21,22] Of the three methods, grafting-through is the only technique that guarantees 100% side-chain attachment. Recent work has demonstrated that living ring-opening metathesis polymerization (ROMP) of norbornenyl macromonomers can be used to prepare well-defined bottlebrush polymers with controlled backbone and side-chain molecular weights.[23,24] While a variety of bottlebrush polymers made by the ROMP grafting-through technique have been reported recently, a study of their solution size and conformation has not been reported. Prior small-angle X-ray scattering (SAXS) and SANS studies have focused on bottlebrush polymers prepared by the grafting-from technique.

Additionally, previously reported studies focused on a limited set of materials with typically long backbone degrees of polymerization (DPs) and in some cases neglected to measure the absolute molecular weight of both the side chains and polymeric backbone, which is necessary for quantitative analysis and comparison between studies.

Herein, we present SANS studies of bottlebrush polymers in solution with systematically varied backbone and side-chain lengths. In contrast to previous SAXS and SANS studies of bottlebrush polymers,[15,18] we focus on bottlebrush polymers made via a grafting-though approach. Absolute molecular weights for the side chains and overall bottlebrush polymers are determined by a combination of static light scattering and ^{1}H NMR measurements. SANS data are analyzed by Guinier–Porod and cylindrical form factor models to estimate the radius of gyration, elongation, diameter, and persistence length of the bottlebrush polymers in solution. Our SANS measurements and analysis demonstrate a power-law dependence of the bottlebrush polymer cross-sectional area with side-chain DP, in quantitative agreement with previous studies. We find a sphere-to-cylinder transition that has not been reported in previous experimental measurements but is consistent with predictions of recent multiscale molecular simulations of bottlebrush polymers.[25] Temperature changes result in small but significant changes in the overall size of the bottlebrush polymer, and we demonstrate that TEM measurements of bottlebrush polymers adsorbed to a surface are a poor reflection of the size and shape of bottlebrush polymers in solution.

EXPERIMENTAL SECTION

Materials. Unless otherwise noted, all reagents and solvents were purchased from commercial suppliers and used as received. Styrene was passed through a basic alumina column to remove inhibitor before polymerization. Dichloromethane (CH_2Cl_2) was dried over molecular sieves (4 Å). *Exo*-7-oxaicyclo(2,2,1)hept-5-ene-2,3-dicarboxylic anhydride (oxanorbornene) and 4-(2-Hydroxyethyl)-10-oxa-4-azatricyclo-[5.2.1.02,6]dec-8-ene-3,5-dion(oxanorbornene ethanol) (NbCTA, **1**) were prepared as previously described and purified by recrystallization.[26] Modified Grubb's catalyst ((H_2IMes)(pyr)$_2$(Cl)$_2$RuCHPh) was synthesized as previously described.[27]

Norbornene-Functionalized Polystyrene Macromonomer (NbPSN, 2) via RAFT. The synthesis is modified from that in our previous report.[26] Optimized reaction conditions for each molecular weight are detailed in Supporting Information Table S1, and details of the synthesis of NbPS42 are presented here. To a 50 mL round-bottomed flask equipped with a stir bar were added NbCTA **1** (0.114g, 0.193 mmol) and styrene (6.09g, 58.53 mmol), followed by the addition of AIBN (0.00323g, 0.0195 mmol). The reaction flask was purged with three freeze−pump−thaw cycles and then heated to 50 °C in a temperature-controlled oil bath. Every hour an aliquot was taken from the reaction mixture and analyzed by gel permeation chromatography (GPC). After 8.5 h, the reaction was quenched by cooling the reaction flask in a liquid-nitrogen bath and exposing it to air. The polymer was precipitated twice in methanol and collected by filtration. Yield: 0.669 g; M_n = 4900 g mol^{-1} and M_w/M_n = 1.12.

Polystyrene Bottlebrushes (PNb(PSN)M). In a representative procedure, modified Grubb's second-generation catalyst ((H_2IMes)-(pyr)$_2$(Cl)$_2$RuCHPh) (0.44 mg, 0.0412 mmol) was dissolved in anhydrous CH_2Cl_2 in a 5 mL round-bottomed flask equipped with a stir bar. **2** (0.2025 g, 0.0213 mmol) was added to a separate 5 mL round-bottomed flasks equipped with a stir bar that was purged and backfilled with nitrogen three times and then dissolved in anhydrous CH_2Cl_2 (0.5 mL, 0.05 mol/L). The macromonomer solution was transferred to the stirring catalyst solution via syringe. The solution was allowed to stir for 1 h, after which the reaction was quenched by the addition of 100 μL of butyl vinyl ether. GPC confirmed the crude

conversion of macromonomer to be greater than 94% for all PS bottlebrush polymers. The product was recovered by precipitating twice in methanol and collecting by filtration. PNb(PS42)148: $M_{n,GPC}$ = 135.4 kg mol^{-1}, M_w/M_n = 1.52. dn/dc = 0.177 in THF. $M_{w,LS}$ = 1100 kg mol^{-1}. A representative ^{1}H NMR spectra is provided in Supporting Information Figure S1. DSC analysis for all bottlebrush polymers is shown in Supporting Information Figure S2.

INSTRUMENTATION

Gel-Permeation Chromatography (GPC). Polymer molecular weights and molecular weight polydispersities (PDIs) were obtained using an Agilent 1200 module equipped with three PSS SDV columns in series (100, 1000, and 10 000 Å pore sizes), an Agilent variable-wavelength UV/vis detector, a Wyatt technology HELEOS II multiangle laser light scattering (MALLS) detector (λ = 658 nm), and a Wyatt Technology Optilab reX RI detector. This system enables SEC with simultaneous refractive index (SEC-RI), UV/vis (SEC-UV/vis), and MALLS detection. THF was used as the mobile phase at a flow rate of 1 mL/min at 40 °C. For bottlebrush polymer synthesis, macromonomer conversion was determined by comparing the integrated areas corresponding to bottlebrush polymer and unreacted macromonomer. Bottlebrush polymer dn/dc values were calculated by assuming 100% mass recovery and correcting the injected mass to account for unreacted macromonomer and are reported in Table S2.

Nuclear Magnetic Resonance Spectroscopy (NMR). Proton NMR (^{1}H NMR) spectra were recorded using tetramethylsilane as an internal standard in CDCl$_3$ on a 400 MHz Bruker multinuclear spectrometer. Samples were placed in 5 mm o.d. tubes with a concentration of 10 mg/mL.

Small-Angle Neutron Scattering (SANS). Temperature-dependent SANS measurements were performed at the National Institute of Standards and Technology Center for Neutron Research on the NG3 30 m instrument with a neutron wavelength of λ = 6 Å. Three sample−detector distances were used (1.3, 4, and 13 m), providing an overall q range of 0.003 Å^{-1} < q < 0.4 Å^{-1}. Polymer samples were prepared at a mass fraction of 1% in deuterated toluene and allowed to equilibrate at RT for at least 4 h. Temperature control was provided by a water circulation bath, and the actual sample temperatures were measured using a thermocouple in thermal contact with the samples. Samples were allowed to equilibrate at each temperature for at least 1 h. For the temperature series data, temperature set points were input as 10, 25, 40, 55, 70, and 85 and were measured to be 11, 25, 40, 54, 68, and 83 °C, respectively. Scattering data were corrected for the solvent baseline with a scale factor (0.95−1.02) appropriate for the mass fraction of solvent. Model fitting was performed using NCNR Data Analysis IGOR PRO software[28] and the Guinier−Porod,[29] cylinder,[30] and flexible cylinder[31,32] models.

Transmission Electron Microscopy (TEM). TEM was performed on JEOL 2010 TEM. Polymer solutions (0.1−1 mg/mL polymer in toluene) were drop-cast onto carbon grids, dried, and stained with RuO$_4$ for 30−90 min prior to imaging.

RESULTS

Bottlebrush Polymer Synthesis. The grafting-through approach enables the preparation of a systematic series of fully grafted bottlebrush polymers with varying backbone and side-chain lengths. As shown in Scheme 1, PS bottlebrush polymers are prepared in two steps. First, PS macromonomers NbPSN (**2**) with a degree of polymerization N are synthesized via

Scheme 1. Synthesis of PS Macromonomers by RAFT Followed by Grafting-Through Synthesis of PS Bottlebrush Polymers via ROMP[a]
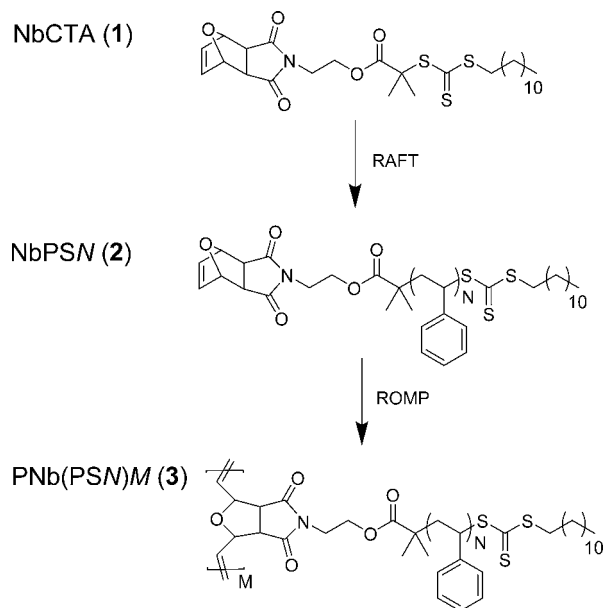
[a]Final PS bottlebrush polymers PNb(PSN)M have PS side chains with a degree of polymerization N and a backbone with a degree of polymerization M.

RAFT using a norbornene-functionalized chain-transfer agent (NbCTA, **1**). PS bottlebrush polymers are subsequently prepared by ROMP of NbPSN macromonomers. The resulting PS bottlebrush polymers have side-chain molecular weights of M_w ranging from 2.3 to 6.9 kg mol^{-1}, corresponding to side-chain DPs from 14 to 54 and overall molecular weights from 36 to 3140 kg mol^{-1}, corresponding to backbone degrees of polymerization DP from 10 to 250 (Table 1). Bottlebrush polymer polydispersities (PDIs) range from 1.2 to 2.3, with broader molecular weight distributions for larger PS side chains.

Table 1. Properties of PS Bottlebrush Polymers PNb(PSN) M, Where N Denotes the Side Chain DP and M Denotes the Backbone DP

	side chain			bottlebrush		
	M_w (kg/mol)[a]	DP	PDI[b]	M_w (kg/mol)[c]	DP[d]	PDI[e]
PNb(PS14)45	2.3	14	1.15	105.0	45	1.16
PNb(PS14)264	2.3	14	1.15	881.0	260	1.67
PNb(PS20)11	3.1	20	1.18	36.6	11	1.23
PNb(PS20)15	3.1	20	1.18	63.0	15	1.65
PNb(PS24)120	3.6	24	1.16	453.0	120	1.22
PNb(PS42)148	5.6	42	1.14	1100.0	150	1.52
PNb(PS54)216	6.9	54	1.12	3140.0	220	1.96

[a]M_w by GPC relative to monodisperse PS standards. Measured values are in good agreement with ^{1}H NMR measurements (Supporting Information Table S1). [b]From GPC relative to monodisperse PS standards. [c]M_w calculated from GPC light-scattering analysis. [d]Calculated using number-averaged molecular weights M_n for side chains and bottlebrush polymer. [e]From GPC relative to monodisperse PS standards. PDI values from light-scattering analysis are comparable and provided in Supporting Information Table S2.

We note that the side chains are spaced by five carbon atoms and one oxygen atom belonging to the bottlebrush poly-(oxanorbornene) backbone, roughly tripling the separation between grafted chains previously analyzed by SAXS and SANS.[18,33−35] Also, all bottlebrush polymer side chains are terminated by trithiocarbonate chain-transfer-agent (CTA) end groups. Although the scattering-length-density contrast for the trithiocarbonate group relative to that of d_8-toluene is greater than that for polystyrene, the mass content is relatively small. For the shortest PS side chain with a DP of 14, the mass content of the trithiocarbonate end group is roughly a mass fraction of 8%. Differences in the scattering-length density of the end group and styrene repeat unit are neglected in the modeling and analysis of SANS data.

For quantitative SANS analysis, accurate measurements of the absolute molecular weight of bottlebrush polymers and bottlebrush polymer side chains are needed. The PS side-chain molecular weight and PDI were obtained by size-exclusion chromatography analysis calibrated by a set of monodisperse PS standards. Measured values were in good agreement with ^{1}H NMR measurements of side-chain DP (Supporting Information Figure S1 and Table S2). The absolute molecular weight of bottlebrush polymers was measured by static light scattering measurements. The use of a linear PS calibration curve significantly underestimates the true molecular weight of PS bottlebrush polymers (Supporting Information Table S2). This reflects the more compact structure of PS bottlebrush polymers in solution compared to that of linear PS with a comparable molecular weight.

Small-Angle Neutron Scattering (SANS) Measurements and Analysis. SANS measurements were carried out on solutions of bottlebrush polymer at 1 wt % in deuterated toluene (d_8-tol), a good solvent for the polystyrene side chains and the polynorbornene backbone. SANS analysis was performed over a q range of 0.008 Å^{-1} up to approximately 0.4 Å^{-1}. This broad q range provides information on the structure of bottlebrush polymers on multiple length scales. Roughly, the low-q region (q = 0.008−0.02 Å^{-1}) gives information on the overall size of the bottlebrush polymer, the mid-q region (q = 0.02 − 0.1 Å^{-1}) provides information about the cross-sectional size and stiffness, and the high-q region (q > 0.1 Å^{-1}) is indicative of thermal fluctuations on the molecular level.

A comparison of the scattering intensity for bottlebrush polymers with varying side-chain lengths and backbone lengths provides qualitative information about the bottlebrush polymer size and cross-sectional area. As shown in Figure 2, the SANS data for a series of bottlebrush polymers with similar side-chain lengths (DP = 14−20) and varying backbone lengths (DP = 11−264) overlap in the mid-q region but diverge in the low-q region, with larger bottlebrush polymers exhibiting an increased low-q scattering intensity. This indicates qualitatively that the series of bottlebrush polymers have similar cross-sectional areas and stiffnesses but differ in overall size. For a series of bottlebrush polymers with long backbone lengths and varying side-chain lengths, differences in the neutron scattering intensity are observed in the low-q and mid-q regions, indicating both cross-sectional areas and overall size changes for this series of polymers.

The slope at low q provides information on polymer conformation. Plateaus indicate globular or spherical particles, as observed for PNb(PS20)15. Alternatively, an increasing slope at low q indicates an elongated shape. PNb(PS14)264
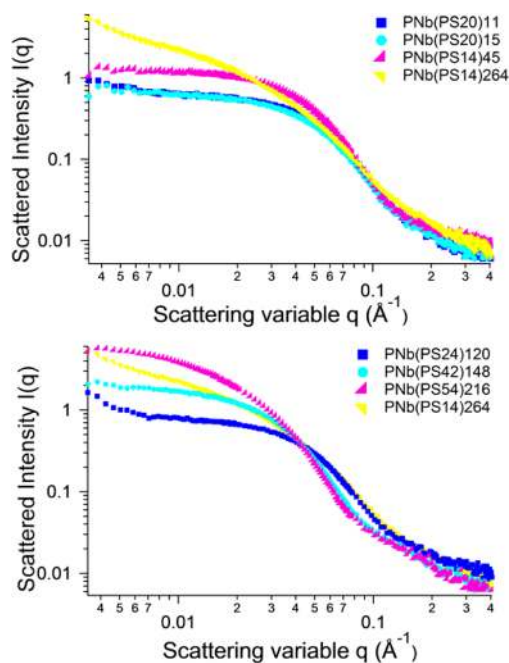
Figure 2. SANS scattering intensity for bottlebrush polymers with similar side-chain molecular weights (2.3−3.1 kg mol⁻¹) (top) overlapping in the mid-q region (0.03 Å⁻¹ > q > 0.1 Å⁻¹), indicative of similar cross-sectional areas. Bottlebrush polymers with long backbones (backbone DP >100) and varying side-chain lengths (bottom) do not overlap in the mid-q region, and the intensity at low q (q < 0.03 Å⁻¹) is greater for bottlebrush polymers with larger backbone DP and/or longer side chains, indicative of a larger overall size.

and PNb(PS54)216 have the greatest backbone DP values, and the slope in the low-q region of the scattering intensity indicates qualitatively that they are more elongated in solution than in the rest of the series. In some cases, such as PNb(PS24)120, a sharp upturn at very low q (q < 0.07 Å⁻¹) reflects the presence of polymer aggregates. For example, both PNb(PS20)15 and PNb(PS14)264 exhibit small degrees of aggregation in solution. In all cases, the amount of aggregation is minor and the data can be fit to a model for a single molecular form factor.

To obtain a quantitative measure of the bottlebrush solution size and conformation, SANS data were first fit to a Guinier−Porod model[29] (Figure 3). This is an empirical model applicable to objects of arbitrary shape and provides an estimate of the radius of gyration, R_g, and dimension parameter, s. As shown in Table 2, results from the Guinier−Porod model give R_g values in the range of 28−49 Å for PS bottlebrush polymers studied. This is much smaller than expected for the overall size of bottlebrush polymers with large backbone DPs but is consistent with the expected cross-sectional area. As shown in Figure 4 and Table 2, the R_g estimate from the Guinier−Porod model trends with the side-chain DP but is independent of the backbone DP. From this, we conclude that the R_g value from the Guinier−Porod model reflects the cross-sectional area and provides an estimate of the bottlebrush polymer radius, not the overall size of the molecule. This is further supported by comparison with model fitting using cylindrical form factors, as discussed below.

Dimension parameter s reflects the shape of the molecule: s = 0 corresponds to a spherical molecule, and s = 1 indicates that the molecule is elongated or rodlike. As shown in Figure 4 and
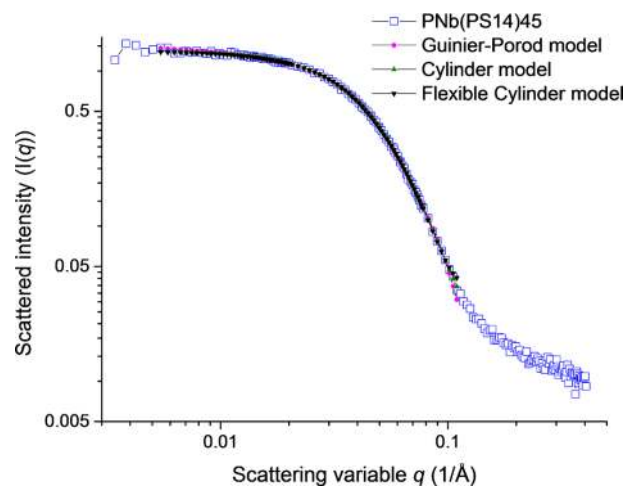

Figure 3. Poly(PS14)45 SANS data and model fits for Guinier−Porod, rigid cylinder, and flexible cylinder models. All models are fit for 0.004 Å⁻¹ < q < 0.09 Å⁻¹.

Table 2. Results from the Guinier−Porod Model for the Radius of Gyration, R_g, and Dimension Parameter, s^a

sample	R_g (Å)	s
PNb(PS14)45	34.2 ± 0.2	0.06 ± 0.01
PNb(PS14)264	27.2 ± 0.3	0.77 ± 0.01
PNb(PS20)11	28.3 ± 0.3	0.07 ± 0.01
PNb(PS20)15	27.9 ± 0.3	0.11 ± 0.01
PNb(PS24)120	31.3 ± 0.3	0.11 ± 0.01
PNb(PS42)148	44.3 ± 0.2	0.19 ± 0.01
PNb(PS54)216	48.9 ± 0.3	0.52 ± 0.01

^{a}Statistical uncertainties correspond to one standard deviation.

Table 2, the dimension parameter is roughly 0.1 for bottlebrush polymers with short backbones (DP < 120) but increases significantly with backbone DP greater than 120. Dimension parameter s increases from 0.1 to 0.7 as the backbone DP increases from 120 to 250. Thus, the Guinier−Porod model indicates an increasing bottlebrush polymer radius with increasing side-chain molecular weight and increasing polymer elongation with backbone repeat units (Figure 4).

More detailed information on bottlebrush polymers can be extracted using rigid and flexible cylinder models for the scattering form factor.[28] The former model approximates individual bottlebrush polymers as rigid cylinders in solution, and the latter assumes that they are flexible cylinders, characterized by a Kuhn step length of λ_k. The rigid cylinder model gives estimates of the radius, R, and length, L, only, and the flexible cylinder model gives estimates of the radius, R_c, in addition to the contour length, L_c, and Kuhn step length, λ_k. The flexible cylinder model has been used in previous SANS and SAXS studies of bottlebrush polymers.[15,18,33] Results from the analysis of the present SANS data by cylinder and flexible cylinder models are shown in Table 3 and Figure 5. The cylinder models are in good agreement, with a longer contour length L_c for the flexible cylinder model compared to the length L of the rigid cylinder model, as expected. The radii range from roughly 25−50 Å and increase with side-chain DP, consistent with the R_g values from the Guinier−Porod model.

The rigid cylinder length L and contour length L_c are both highly dependent on the backbone DP, with a strong increase above a backbone DP of approximately 120. Below a DP of 90,
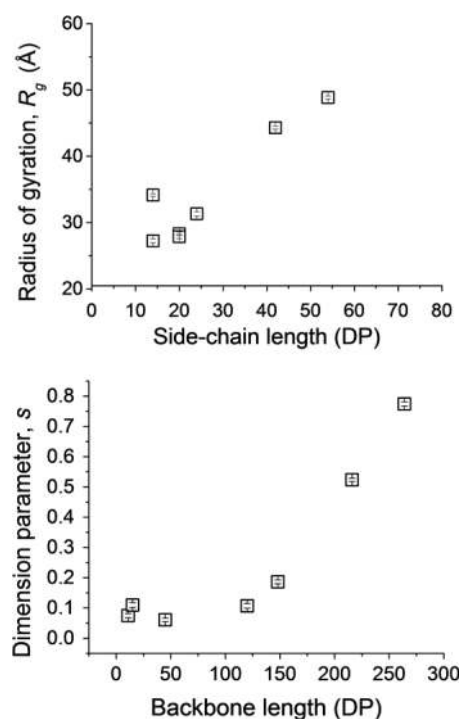
Figure 4. Analysis by the Guinier–Porod model indicating an increase in the radius of gyration, R_g, with side-chain length (top) and a strong increase in the dimension parameter, s, as a function of backbone length for backbone DPs greater than 120 (bottom). Standard deviations (shown) are smaller than data points. Statistical uncertainties correspond to one standard deviation.

Figure 5. Results from cylinder ($\square$) and flexible-cylinder ($\bigcirc$) models. Radii, R, (top) increase with side-chain length. Length, L, ($\square$) and contour length, L_c, ($\bigcirc$) (bottom) are dependent on the backbone length. Standard deviations (shown) are typically smaller than data points. Statistical uncertainties correspond to one standard deviation.

the cylinder lengths are roughly independent of the backbone DP. This is inconsistent with a cylindrical shape and suggests a spherical globule conformation of the bottlebrush polymer overall, not an extended cylinder. This is also predicted by the Guinier–Porod model, which gives a small dimension parameter s for all bottlebrush polymers with backbone DPs of less than 120 (Table 2). We note that for these samples the values of the Kuhn length λ_k determined from the flexible cylinder model are equal to twice the cylinder radius; equivalently, the bottlebrush polymer persistence length ($2l_p = \lambda_k$) is roughly equal to the bottlebrush polymer radius. The same is true for bottlebrush polymers PNb(PS24)120 and PNb(PS42)148, which are only weakly extended ($s = 0.11$ and 0.19, respectively). Thus, for bottlebrush polymers with backbone DPs of less than 150, λ_k does not reflect the Kuhn length of the poly(oxanorbornene) backbone but rather reflects
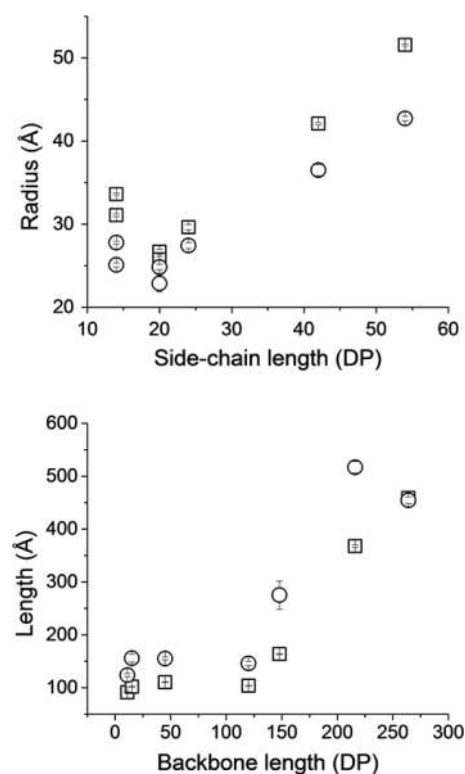
the characteristics of the bottlebrush polymer diameter and cross-sectional area.

Bottlebrush polymers with the largest backbone DPs, PNb(PS14)264 and PNb(PS54)216, have an extended cylinder conformation, and λ_k reflects the poly(oxanorbornene) backbone Kuhn length. For these two polymers, λ_k increases weakly with increasing side-chain length; λ_k increases by 13% with an almost 4-fold increase in the side-chain DP. Although we cannot draw strong conclusions from two samples, we note that molecular simulations predict a modest increase in persistence length with increasing side-chain DP.[25] We note that the λ_k values from our analysis are significantly smaller than those previously measured for polystyrene[33] and poly(butylacrylate) bottlebrush polymers.[15,18] This may be due to the much greater spacing between side chains for the present samples with a poly(oxanorbornene) backbone as opposed to the methacrylic

Table 3. Results from Rigid Cylinder and Flexible Cylinder Models[a]

	rigid cylinder		flexible cylinder		
polymer	R (Å)	L (Å)	R_c (Å)	L_c (Å)	λ_k (Å)
PNb(PS14)45	31.1 ± 0.2	110.5 ± 0.6	27.8 ± 0.2	155.2 ± 2.8	66.9 ± 2.0[b]
PNb(PS14)264	28.9 ± 0.1	443.0 ± 5.5	25.1 ± 0.2	454.6 ± 6.2	113.3 ± 3.7
PNb(PS20)11	26.7 ± 0.3	91.3 ± 0.8	24.8 ± 0.3	123.8 ± 2.9	54.3 ± 2.4[b]
PNb(PS20)15	25.7 ± 0.4	101.8 ± 0.9	22.9 ± 1.0	155.9 ± 7.3	51.1 ± 7.1[b]
PNb(PS24)120	29.6 ± 0.3	104.0 ± 0.9	27.4 ± 0.3	146.1 ± 3.6	58.4 ± 3.2[b]
PNb(PS42)148	42.1 ± 0.2	163.5 ± 0.9	36.5 ± 0.7	275.1 ± 26.6	68.8 ± 12.1[b]
PNb(PS54)216	51.6 ± 0.1	367.8 ± 2.1	42.7 ± 0.3	516.8 ± 10.8	129.1 ± 5.8

[a]Statistical uncertainties correspond to one standard deviation. [b]For these samples, the λ_k values do not reflect the true Kuhn length of the bottlebrush polymer backbone; see the text for a more detailed discussion.

backbone in the materials studied by Schmidt et al.[35,36] and Rathgeber et al.[15,37] The side chains in the present study are separated by five carbon atoms and one oxygen atom along the poly(oxanorbornene) backbone, whereas for a methacrylic backbone the side chains are separated by only two carbon atoms.

The changes in the bottlebrush polymer radius and overall size were measured as a function of temperature to determine how the side chain and backbone conformations change with solvent quality. (Temperature-dependent SANS data is provided in Supporting Information Figure S3.) Five bottlebrush polymers were analyzed at 11, 25, 40, 54, 68, and 83 °C in d_8-toluene, a roughly athermal solvent for polystyrene for the measured temperature range.[38] Linear PS in toluene shows a weak temperature dependence of the intrinsic viscosity with temperature in toluene, with increased chain swelling at elevated temperatures.[38,39] For cylindrical bottlebrush polymers (PNb(PS24)120 and PNb(PS54)216), we observed modest backbone elongation with increasing temperature, between 3 and 7% increases in length, as determined from rigid cylinder models (Figure 6). The radii of bottlebrush polymers remained relatively constant with increasing temperature.
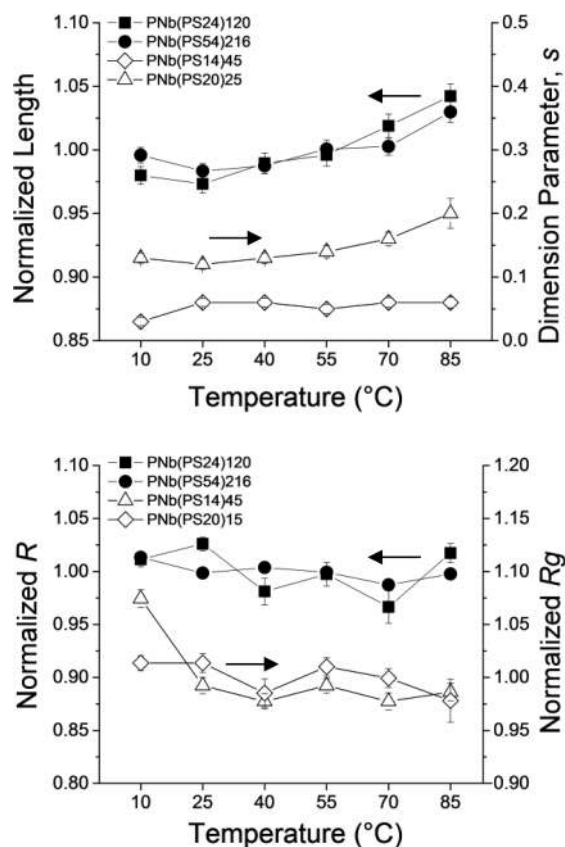

Figure 6. Normalized length (top, solid markers), dimension parameter (top, open markers), cylinder radii (bottom, solid markers), and Guinier–Porod R_g (bottom, open markers) for bottlebrush polymers. Bottlebrush polymers with backbone DPs greater than 100 (PNb(PS24)120 and PNb(PS54)216) were analyzed by the cylinder model whereas shorter bottlebrush polymers PNb(PS14)45 and PNb(PS20)15 were analyzed by the Guinier–Porod model. PNb-(PS24)120 and PNb(PS54)216 show modest elongation with increasing temperature. Values for length, L_c, radius, R, and radius of gyration, R_g, are normalized with respect to the average length or radius for each polymer; error bars represent the model fit tolerance.

TEM. For comparison to the bottlebrush polymer sizes calculated from SANS analysis, select bottlebrush polymers were visualized by conventional TEM. As shown in Figure 7, TEM reveals particles that are spherical in shape. Bottlebrush polymers with longer backbone DPs (PNb(14)264 and PNb(54)216) have a more ellipsoidal shape, but no cylindrical molecules are observed. Precise quantitative values are difficult to extract from TEM analysis, but image analysis provided estimates for the average molecular diameter. Particle size measurements by TEM give larger values for the average molecular size than do SANS measurements. For example, PNb(PS20)15 and PNb(PS14)264 were measured to be approximately 22 and 43 nm in length by TEM compared to 10 and 44 nm by SANS.

■ DISCUSSION

The measurements reported here provide quantitative information about the solution conformation of bottlebrush polymers. Consistent with previous SANS and SAXS measurements,[15,33,34] we observe a power-law dependence of the side-chain size with side-chain DP, $R \approx DP^\nu$. Using R_g values from the Guinier–Porod model, we found the value of exponent ν to be 0.39. Using cylinder radius R from the cylindrical form factor models provides a slightly larger exponent of 0.42. As noted above, SANS data have a contribution from the trithiocarbonate CTA pendant on each side chain. The effect of the CTA will be more pronounced for shorter side chains. Neglecting the bottlebrush polymers with the shortest side chains, we find exponents of 0.57 and 0.71 from Guinier–Porod and cylindrical form factor models. These numbers are consistent with previous studies and suggest a 2D or 3D self-avoiding walk conformation of the polymeric side chains.[15,33,34] Additionally, we can estimate the length per repeat unit for the polystyrene side chains using the side-chain DP and values for R or R_g. Our analysis indicates that side chains have an average length per repeat unit that is greater than 1 nm in all cases, indicating that they are strongly stretched.

The analysis of SANS data by both Guinier–Porod and cylindrical form factor models predicts a sphere-to-cylinder transition with increasing backbone DP, as shown schematically in Figure 8. The data for PS bottlebrush polymers show a more elongated solution conformation for PS bottlebrush polymers with DPs greater than 120, whereas bottlebrush polymers with smaller backbone DPs are roughly spherical globules in solution. This is consistent with recent molecular simulations[25] and previous experimental observations.[24,40]

This conformational transition can be attributed to both side-chain stretching and end effects, which are more pronounced for shorter backbone lengths. As shown schematically in Figure 8, side chains near the terminal ends of the backbone are free to rotate and form a spherical cap. For shorter bottlebrush polymer backbones, the molecular structure resembles a globular or spherical conformation. In contrast, bottlebrush polymers with longer backbones (greater than the average length of the highly stretched side chains) have an extended cylinderlike conformation. Our results indicate that PNb-(PS14)264 and PNb(PS54)216 are in the cylindrical regime whereas PNb(PS24)120 and PNb(PS42)148 are only slightly extended. All other bottlebrush polymers are spherical globules in solution.

Our observations are in agreement with early studies of bottlebrush polymers prepared by free-radical polymerization that concluded bottlebrush polymers become more extended
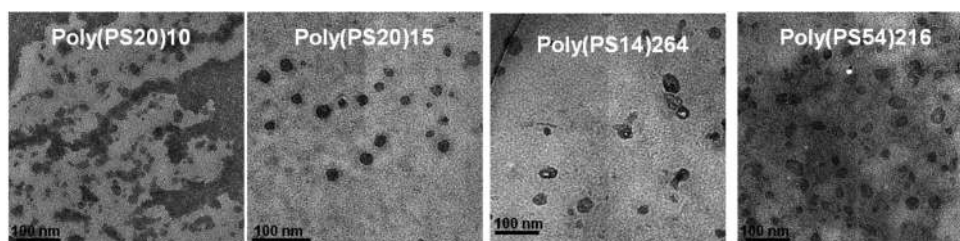
Figure 7. TEM micrographs of select PS bottlebrush polymers adsorbed to a surface. Scale bars (shown) are 100 nm.
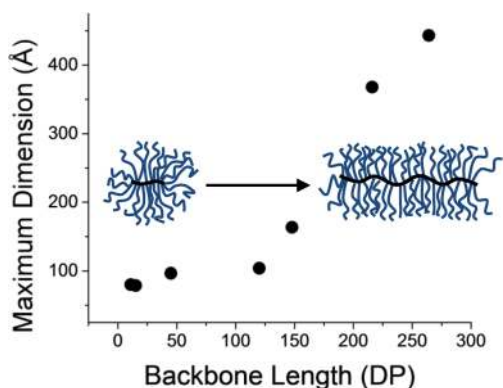

Figure 8. Schematic for the conformation of bottlebrush polymers for small (left) and large (right) backbone DPs and a plot of the maximum dimension for both spherical and cylindrical bottlebrush polymers. The maximum dimension is defined as the diameter of spherical bottlebrush polymers and the backbone length of cylindrical bottlebrush polymers.

for backbone degrees of polymerization greater than 10.[34] Other examples include bottlebrush polymers with short backbone and side-chain DPs analyzed by SANS and TEM measurements of bottlebrush polymers made by grafting-through.[24] Monte Carlo simulations by Binder et al.[25] predict a total radius of gyration R_g comparable to the side-chain size for backbone DPs of less than 100.

Thus, the use of a cylindrical form factor is inappropriate for bottlebrush polymers with smaller backbone DPs. To understand the sphere-to-cylinder conformational transition in bottlebrush polymers, we define the maximum dimension as the diameter for spherical bottlebrush polymers and the length for cylindrical bottlebrush polymers. We can estimate the maximum dimension for bottlebrush polymers in solution using the Guinier−Porod model (diameter $D = 2(2^{1/2})R_g$) for bottlebrush polymers with backbone DPs of less than 120 and a cylinder model length L for bottlebrush polymers with backbone DPs greater than 120 (Figure 8). As shown in Figure 8, this analysis predicts the maximum dimension to be independent of backbone length below backbone DPs of 120, where side-chain stretching determines the size of the bottlebrush polymer. Above a backbone DP of roughly 120, the maximum dimension increases with backbone DP. Although we observe this conformational transition at a backbone DP of roughly 120, this transition will generally depend on the side-chain length, flexibility, and grafting density.

Our results further indicate that the backbone is not fully stretched, with lengths of backbone per monomer repeat unit, l_b, of roughly 0.18 nm $\pm$ 0.05 nm using contour length values from the flexible cylinder model for the bottlebrush polymers with DPs greater than 120. By comparison, the theoretical length for a fully extended backbone is roughly 0.5 nm per

backbone unit.[40] For bottlebrush polymers with backbone DPs greater than 120, temperature changes are found to affect only the backbone length, not the side-chain length or bottlebrush polymer radius. This suggests that side chains are highly stretched at all temperatures whereas the backbone has more flexibility and elongates with increasing temperature.

TEM analysis gives a poor reflection of the solution conformation of bottlebrush polymers. In all cases, we observe spherical particles with sizes in the range of 20−40 nm. The discrepancy between SANS and TEM measurements of molecular size and shape may be due to a combination of effects: molecular aggregation during TEM sample preparation, side-chain collapse, and deformation on adsorption to a solid surface.

■ ASSOCIATED CONTENT

ⓢ Supporting Information
Additional material characterization, ^{1}H NMR data, DSC data, and additional SANS traces. This material is available free of charge via the Internet at http://pubs.acs.org.

■ AUTHOR INFORMATION

Corresponding Author
*E-mail: rafaelV@rice.edu.

Notes
The authors declare no competing financial interest.

■ ACKNOWLEDGMENTS

■ REFERENCES

(1) Johnson, J. A.; Lu, Y. Y.; Burts, A. O.; Lim, Y.-H.; Finn, M. G.; Koberstein, J. T.; Turro, N. J.; Tirrell, D. A.; Grubbs, R. H. *J. Am. Chem. Soc.* **2010**, *133*, 559.
(2) Xia, Y.; Li, Y.; Burts, A. O.; Ottaviani, M. F.; Tirrell, D. A.; Johnson, J. A.; Turro, N. J.; Grubbs, R. H. *J. Am. Chem. Soc.* **2011**, *133*, 19953.

(3) Rosenhahn, A.; Schilp, S.; Kreuzer, H. J.; Grunze, M. *Phys. Chem. Chem. Phys.* **2010**, *12*, 4275.

(4) Miki, K.; Kimura, A.; Oride, K.; Kuramochi, Y.; Matsuoka, H.; Harada, H.; Hiraoka, M.; Ohe, K. *Angew. Chem., Int. Ed.* **2011**, *50*, 6567.

(5) Miki, K.; Oride, K.; Kimura, A.; Kuramochi, Y.; Matsuoka, H.; Harada, H.; Hiraoka, M.; Ohe, K. *Small* **2011**, *7*, 3536.

(6) Zhao, P.; Liu, L.; Feng, X.; Wang, C.; Shuai, X.; Chen, Y. *Macromol. Rapid Commun.* **2012**, *33*, 1351.

(7) Zou, J.; Jafr, G.; Themistou, E.; Yap, Y.; Wintrob, Z. A. P.; Alexandridis, P.; Ceacareanu, A. C.; Cheng, C. *Chem. Commun.* **2011**, *47*, 4493.

(8) Rao N, V.; Mane, S.; Kishore, A.; Das Sarma, J.; Shunmugam, R. *Biomacromolecules* **2011**, *13*, 221.

(9) Bolton, J.; Rzayev, J. *ACS Macro Lett.* **2011**, *1*, 15.

(10) Zhang, M.; Breiner, T.; Mori, H.; Müller, A. H. E. *Polymer* **2003**, *44*, 1449.

(11) Nese, A.; Li, Y.; Averick, S.; Kwak, Y.; Konkolewicz, D.; Sheiko, S. S.; Matyjaszewski, K. *ACS Macro Lett.* **2011**, *1*, 227.

(12) Cheng, C.; Khoshdel, E.; Wooley, K. L. *Macromolecules* **2007**, *40*, 2289.

(13) Ruhs, P. A.; Adamcik, J.; Bolisetty, S.; Sanchez-Ferrer, A.; Mezzenga, R. *Soft Matter* **2011**, *7*, 3571.

(14) Feuz, L.; Strunz, P.; Geue, T.; Textor, M.; Borisov, O. *Eur. Phys. J. E* **2007**, *23*, 237.

(15) Rathgeber, S.; Pakula, T.; Wilk, A.; Matyjaszewski, K.; Lee, H.-i.; Beers, K. L. *Polymer* **2006**, *47*, 7318.

(16) Cheng, G.; Hua, F.; Melnichenko, Y. B.; Hong, K.; Mays, J. W.; Hammouda, B.; Wignall, G. D. *Eur. Polym. J.* **2008**, *44*, 2859.

(17) Neugebauer, D.; Zhang, Y.; Pakula, T.; Sheiko, S. S.; Matyjaszewski, K. *Macromolecules* **2003**, *36*, 6746.

(18) Rathgeber, S.; Pakula, T.; Wilk, A.; Matyjaszewski, K.; Beers, K. L. *J. Chem. Phys.* **2005**, *122*, 124904.

(19) Lee, H.-i.; Pietrasik, J.; Sheiko, S. S.; Matyjaszewski, K. *Prog. Polym. Sci.* **2010**, *35*, 24.

(20) Sheiko, S. S.; da Silva, M.; Shirvaniants, D.; LaRue, I.; Prokhorova, S.; Moeller, M.; Beers, K.; Matyjaszewski, K. *J. Am. Chem. Soc.* **2003**, *125*, 6725.

(21) Gao, H.; Matyjaszewski, K. *J. Am. Chem. Soc.* **2007**, *129*, 6633.

(22) Cerit, N.; Cakir, N.; Dag, A.; Sirkecioglu, O.; Durmaz, H.; Hizal, G.; Tunca, U. *J. Polym. Sci., Part A: Polym. Chem* **2011**, *49*, 2850.

(23) Li, A.; Ma, J.; Sun, G.; Li, Z.; Cho, S.; Clark, C.; Wooley, K. L. *J. Polym. Sci., Part A: Polym. Chem* **2012**, *50*, 1681.

(24) Li, Z.; Ma, J.; Lee, N. S.; Wooley, K. L. *J. Am. Chem. Soc.* **2011**, *133*, 1228.

(25) Hsu, H.-P.; Paul, W.; Rathgeber, S.; Binder, K. *Macromolecules* **2010**, *43*, 1592.

(26) Li, X.; Prukop, S. L.; Biswal, S. L.; Verduzco, R. *Macromolecules* **2012**, *45*, 7118.

(27) Sanford, M. S.; Love, J. A.; Grubbs, R. H. *Organometallics* **2001**, *20*, 5314.

(28) Kline, K. R. *J. Appl. Crystallogr.* **2006**, *39*, 895.

(29) Hammouda, B. *J. Appl. Crystallogr.* **2010**, *43*, 716.

(30) Guinier, A.; Fournet, G. *Small-Angle Scattering of X-rays*; Wiley: New York, 1955.

(31) Pedersen, J. S.; Schurtenberger, P. *Macromolecules* **1996**, *29*, 7602.

(32) Chen, W.-R.; Butler, P. D.; Magid, L. J. *Langmuir* **2006**, *22*, 6539.

(33) Zhang, B.; Gröhn, F.; Pedersen, J. S.; Fischer, K.; Schmidt, M. *Macromolecules* **2006**, *39*, 8440.

(34) Wataoka, I.; Urakawa, H.; Kajiwara, K.; Schmidt, M.; Wintermantel, M. *Polym. Int.* **1997**, *44*, 365.

(35) Wintermantel, M.; Gerle, M.; Fischer, K.; Schmidt, M.; Wataoka, I.; Urakawa, H.; Kajiwara, K.; Tsukahara, Y. *Macromolecules* **1996**, *29*, 978.

(36) Neiser, M. W.; Okuda, J.; Schmidt, M. *Macromolecules* **2003**, *36*, 5437.

(37) Börner, H. G.; Duran, D.; Matyjaszewski, K.; da Silva, M.; Sheiko, S. S. *Macromolecules* **2002**, *35*, 3387.

(38) Berry, G. C. *J. Chem. Phys.* **1967**, *46*, 1338.

(39) Wagner, H. L. *J. Phys. Chem. Ref. Data* **1985**, *14*, 1101.

(40) Li, Z.; Zhang, K.; Ma, J.; Cheng, C.; Wooley, K. L. *J. Polym. Sci., Part A: Polym. Chem.* **2009**, *47*, 5557.